FINITE ELEMENT SIMULATION OF TIG WELDING: STRUCTURAL ANALYSIS

Alexandre Campos Bezerra
acbezerra@mecanica.ufu.br

Domingos Alves Rade
domingos@ufu.br

Américo Scotti
ascotti@mecanica.ufu.br

Federal University of Uberlândia – School of Mechanical Engineering,
Av. João Naves de Ávila, 2121, 38400-902, Uberlândia/MG - Brazil

Abstract. *Welding process involves thermal cycles which generate high temperature gradients and, consequently, residual stresses. Very often, these stresses are undesirable, requiring thermal treatments for stress relief. However, in many cases, this type of treatment becomes technically and economically unsuitable. Thus, one must take into account these stresses in the design of welded components. Several researchers have carried out studies in order to evaluate and minimize the occurrence of welding residual stresses. In this paper, finite element structural simulations are performed to evaluate the residual stresses generated during a TIG welding process without filler metal in a stainless steel AISI 316L plate. The results of thermal analysis presented in a companion paper are used, in terms of the temperature field as a function of time. The finite element commercial code ANSYS® is used. The plate is meshed using solid elements. For a better representation of real welding conditions, temperature-dependent thermo-mechanical properties are considered, which, together with plasticity and hardening effects, lead to a non-linear analysis. Static analysis is performed for each time step throughout the welding process. The numerical results obtained are shown to be in good agreement with results found in the literature, which demonstrates the suitability and efficiency of the finite element method for the prediction of welding residual stresses.*

Keywords*: TIG welding, numerical simulation, stress distribution, structural modeling*

1. Introduction

Welding is very frequently used as a manufacturing process in engineering. It is well known the fact that welding leads to the generation of residual stresses, which are defined by Cullity (1978) as auto-equilibrating stresses that remain in the material in absence of external loads (which include thermal gradients). In the specific case of welding, these stresses are the result of non-uniform plastic strains caused by the elevated temperature gradients and phase transformations that occur during the process.

Generally, these stresses are undesirable due to the possibility of prejudicing the quality of welded components (Parlane *et al.*, 1981). Nevertheless, the minimization or elimination of these stresses is a difficult task and a good practice is to consider them inherently in the design. This way, the characterization of welding residual stresses has been the object of several studies, which use either experimental or numerical methods. It is widely known that experimental methods present critical limitations, such as being costly and time consuming. Moreover, typical drawbacks are that, depending on the particular technique employed, the stress measurements must be performed at one point at a time, can be restricted to specific types of materials and can even provide incorrect results when plastic strain occur. On the other hand, numerical methods for this purpose have been more and more developed, mainly due to the evolution of computational technology, despite the difficulties in achieving accurate modeling of complex phenomena (plasticity behavior, temperature dependence of the material properties, and so on) and difficulties related to the numerical computations themselves (computational cost and convergence problems).

In the scope of numerical methods, several researchers have studied the resolution of the welding structural problem. In the earliest simulations, many simplifications were adopted, such as those used in the study carried out by Kamtekar (1978), which was based on the finite difference method, assuming temperature-independent material properties (except the yield stress) and the determination of the thermal distribution through the simplified analytical formulation of Rosenthal (1941). Papazoglou and Masubuchi (1982), using a 2D finite element model, included the effect of solid phase transformations that occur during the process. Still in 2D models, multi-pass welding was simulated by Free and Goff (1989) and material hardening was included in the modeling by (Hong *et al.*, 1998). More detailed simulations, with 3D complete models, were recently performed (Fricke *et al.*, 2001; Francis, 2002; Depradeux, 2004). However, there is still a lack of information on the capability of these models to characterize the real distributions of welding residual stresses.

In this context, this work seeks to contribute to the resolution of welding structural problems by evaluating the application of Finite Element Method (FEM) and 3D solid modeling for obtaining the residual stresses generated by a TIG welding without filler metal on a stainless steel AISI 316L plate. It is also aimed to characterize the deformed shape of the plate and the transverse displacements to be compared to experimental results extracted from the literature.

2. Structural analisys

The welding structural analysis constitutes an even more difficult problem than the thermal analysis. This is due to different factors, such as a larger number of degrees of freedom and a more complex non-linear behavior. Moreover, there may be numerical instability setbacks due to the fact that the material presents low stiffness at high temperatures. This is, in many cases, the cause for non-convergence.

According to Francis (2002), another very important aspect, which has attracted the attention of the scientific community to a greater extent, is the solid phase transformation. The plastic strain caused by this type of transformation is known as *transformation plasticity*. This strain is irreversible because transformation back to the original phase does not reverse the strain. It may, in fact, increase the strain. The primary mechanism responsible for transformation plasticity is the volume change, which occurs during the phase transformation. Depradeux (2004) points out another feature of the structural analysis: despite of not being a requirement, the mesh used for the structural analysis is generally the same of the thermal analysis. However, the elements have different characteristics, in particular, the number of degrees of freedom.

Like in the thermal analysis, it is possible to solve a 3D complete problem, as well as to use 2D simplified models. Nonetheless, the resolution of the structural problem, when de-coupled of the thermal problem, consists in a static equilibrium analysis for each instant of time considered. This is because, according to Lemaitre and Chaboche (1988), plastic strains can be defined as time-independent irreversible strains. Thus, there is no need to perform time integration in the structural analysis.

The total strain can be expressed as:

$$\varepsilon_{Total} = \varepsilon_e + \varepsilon_{therm} + \varepsilon_p \tag{1}$$

where ε_e is the elastic strain, ε_{therm} is the thermal strain and ε_p is the plastic strain.

The elastic component of strain can be determined directly by the Hooke's law, using the Young modulus, within the range limited by the yield strength of the material (recalling that these properties depend on temperature). The thermal strain is obtained by using the physics law of thermal expansion:

$$\varepsilon_{therm} = \alpha\left(T - T_{ref}\right) \tag{2}$$

where α is the thermal expansion coefficient, T is the current temperature and T_{ref} is the reference temperature at which the expansion is null.

The modeling of plasticity is very complex. Initially, it is necessary to define the elastic domain, which is normally based on the von Mises criterion:

$$\sigma_{vM} - \sigma_y < 0 \tag{3}$$

where σ_y is the yield strength and σ_{vM} is the von Mises equivalent stress, which is defined as (Lemaitre and Chaboche, 1988):

$$\sigma_{vM} = \sqrt{\frac{1}{2}\left[\left(\sigma_1 - \sigma_2\right)^2 + \left(\sigma_2 - \sigma_3\right)^2 + \left(\sigma_3 - \sigma_1\right)^2\right]} \tag{4}$$

where σ_1, σ_2 and σ_3 are the principal stresses. According to the von Mises criterion, plastic strains will be developed when the following condition is satisfied:

$$\sigma_{vM} - \sigma_y = 0 \tag{5}$$

It should be noted that the equivalent stress can never exceed the material yield limit since, in this case, plastic strains would develop instantaneously, thereby reducing the stress to the material yield (Ansys, 1997). The surface represented by Eq. (5) is known as *yield surface*.

The hardening rule describes the changing of the yield surface with progressive yielding, so that the conditions (i.e. stress states) for subsequent yielding can be established. Two hardening rules are available: isotropic hardening and kinematic hardening (Lemaitre and Chaboche, 1988). In isotropic hardening, the yield surface remains centered about its initial centerline and its size increases as the plastic strains evolve (Fig. 1a). This type of hardening is adequate to

represent a monotonic loading, which is analogous to a one-pass welding. Kinematic hardening, on the other hand, assumes that the yield surface remains constant in size, but it translates in stress space with progressive yielding (Fig. 1b). This type of hardening, in association with isotropic hardening, is used to represent the case of multi-pass welding (Murthy *et al.*, 1996).

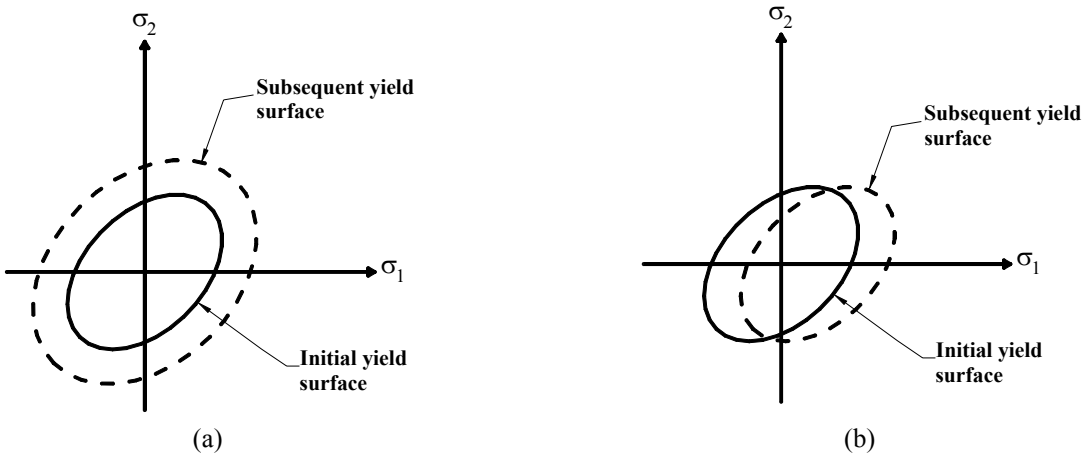

Figure 1. (a) Expansion of yield surface in isotropic hardening and (b) translation of yield surface in kinematic hardening.

3. Numerical Modeling

The numerical modeling was performed using the FE code ANSYS®. The modeled piece is a 250 mm × 160 mm × 10 mm stainless steel AISI 316L plate. It was considered that the material does not suffer any phase transformation in solid state, since it has an austenitic matrix which is stable from room temperature to a value near fusion temperature. It was assumed a multilinear isotropic hardening based on von Mises plasticity criterion. Large strain effects were also taken into account.

The stress-strain curve used as function of temperature, which was obtained experimentally by Depradeux (2004), is illustrated in Fig. 2. Table 1 shows the thermal expansion coefficient and the Young modulus as a function of temperature Depradeux (2004). The Poisson ratio was considered constant and equal to 0.30. Above fusion, it was adopted a very small Young modulus to simulate the low stiffness of the welding pool.

The element used to mesh the model is SOLID45, which is a 3D solid element with eight nodes having three degrees of freedom per node (translations in the nodal *x*, *y* and *z* directions). The meshed model (17,574 nodes) is shown in Fig. 3 and it is the same used for the thermal analysis presented in a companion paper (Bezerra *et al.*, 2005). The plate is supported on three supports situated according to Fig. 4. Therefore, a displacement restriction in *z* direction was imposed at these points on the bottom face of the plate.

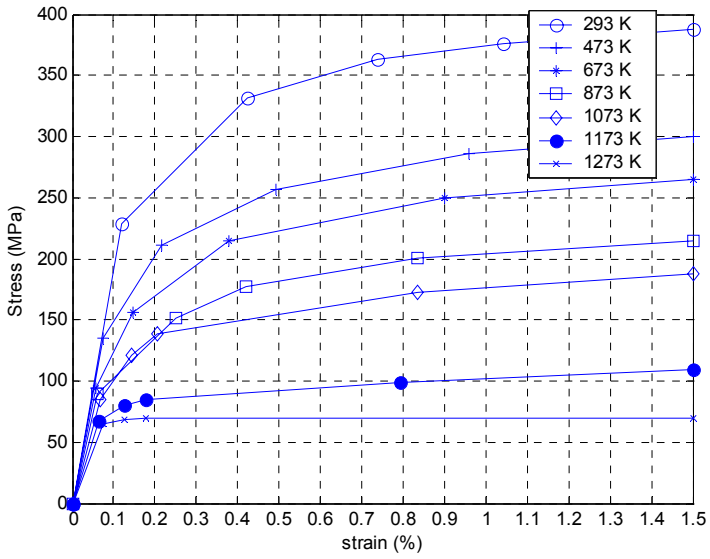

Figure 2. Stress-strain curve as a function of temperature (Depradeux, 2004).

Table 1. Young modulus and thermal expansion coefficient (Depradeux, 2004).

Temperature (K)	Young modulus (GPa)	Thermal expansion coefficient (K^{-1})
293	193,30	15,50
373	-	16,00
473	182,56	-
573	-	17,10
673	161,89	17,50
873	149,80	18,40
973	-	18,70
1073	128,03	19,00
1173	107,10	-
1273	88,70	19,40
1673	-	19,60

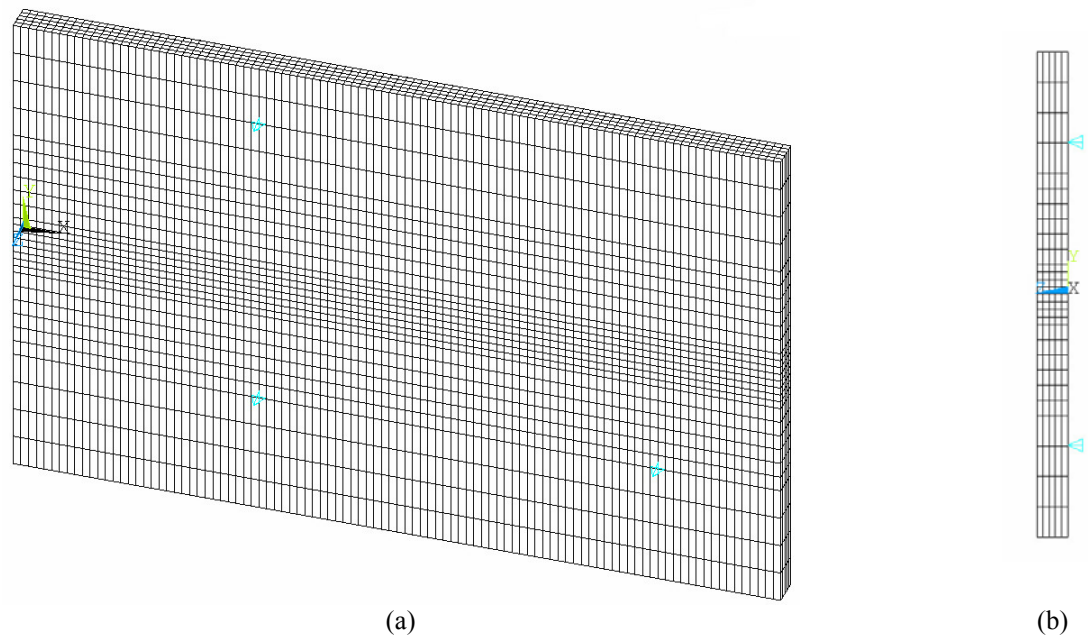

(a) (b)

Figure 3. Finite element mesh of the studied plate (a) and its cross-section view (b).

The welding process simulated was the TIG process. The welding parameters used were: current of 150 A, voltage of 10 V and travel speed of 1 mm/s. A series of static analysis were carried out, in which the time evolution is considered by applying sequentially the transient temperature field by means of load-steps. In this manner, for each instant of time considered, the corresponding temperature field was applied and the new displacement field was determined considering the state of the previous load-step. Room temperature (301 K) was imposed as reference. A routine in MATLAB® was implemented to write an ANSYS® input file, which inputs the results of thermal analysis previously obtained, as described by Bezerra *et al.* (2005).

4. Results

The numerical results obtained were compared to experimental results presented by Depradeux (2004). The transverse displacements were compared using three sections (*S1* to *S3*), according to Fig. 4. The points *P1* to *P6* were used to evaluate, during the welding and the cooling, the transverse displacements on the bottom face as a function of time, while the sections *S1* and *S2* were used to evaluate the final deformed shape on bottom and upper faces. The welding residual stresses were compared at section x=150 mm on the bottom face. The experimental results of residual stress were obtained via X-ray diffraction technique, the transverse displacements via inductive sensors and the final deformed shape by using a feeler gage, all of them obtained by Depradeux (2004).

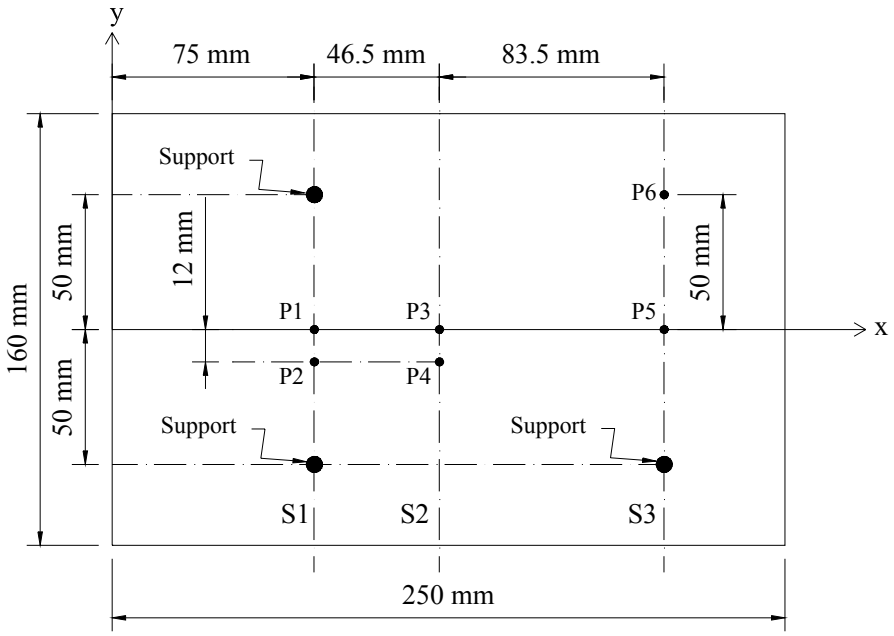

Figure 4. Cross-sections and points used for comparing experimental and numerical results.

Figure 5 shows the numerical and experimental results describing the evolution of the transverse displacements as a function of time for the points indicated in Fig. 4. It is possible to verify a good agreement between the results both during welding (until 230 s) and during cooling. However, during cooling, the numerical results for point *P6* remains constant and equal to zero, while the experimental one suffers a slight drop (about 100μm).

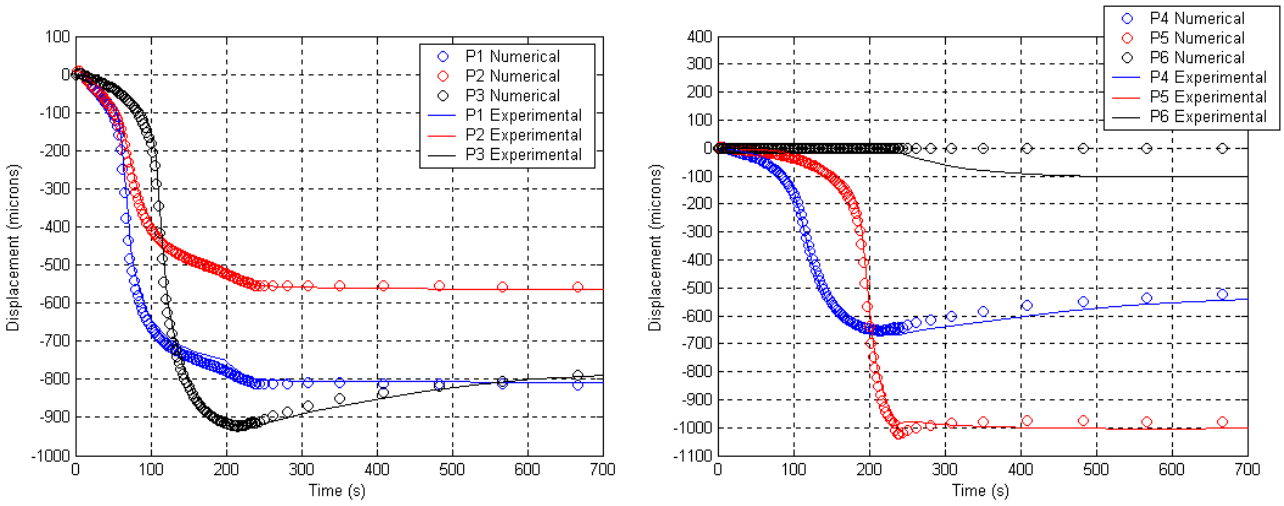

Figure 5. The evolution of the transverse displacement as a function of time at points *P1* to *P6*.

Figure 6 shows a comparison between experimental and numerical results for residual transverse displacements, that is to say, those that remain after complete cooling of the welded piece, in sections *S1* and *S2* for bottom and upper faces. It is clearly verified the occurrence of bending about the *x* axis, which makes the plate to deform into a "V" shape. It can be observed again a satisfactory agreement between numerical and experimental results, mainly for the bottom face. For the upper face, disagreement is noticed only at y=0.

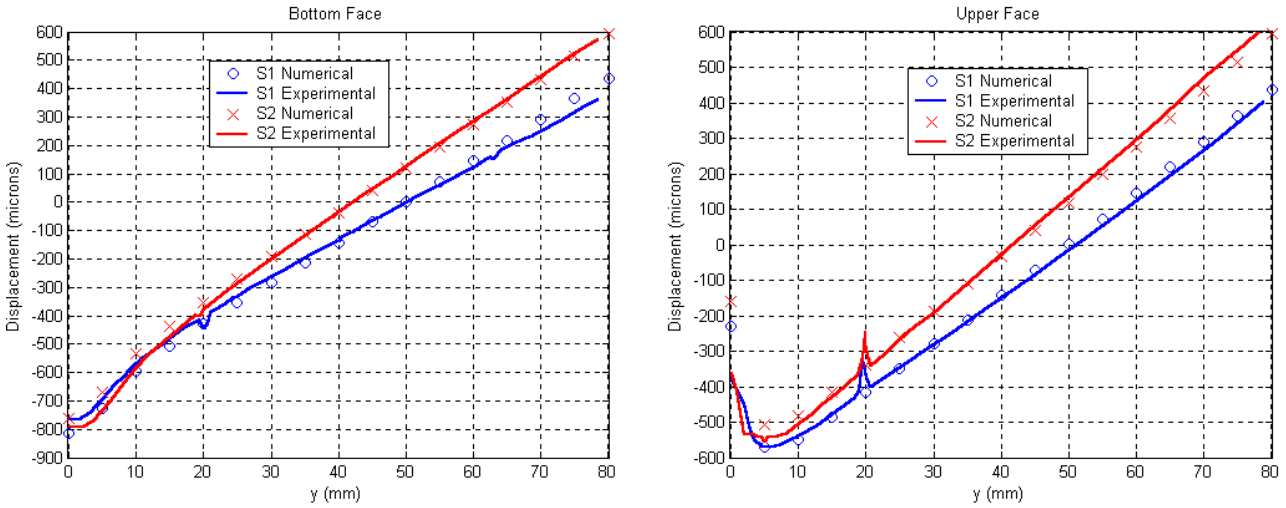

(a) (b)

Figure 6. Final deformed shape of sections *S1* and *S2* on bottom (a) and upper (b) faces.

Figure 7a illustrates the residual transverse displacement field (after cooling) and Fig. 7b depicts the final deformed shape with an amplification of 20 times. Analyzing these results, it is possible to see that bending occurs not only about the *x* axis, but also about the *y* axis.

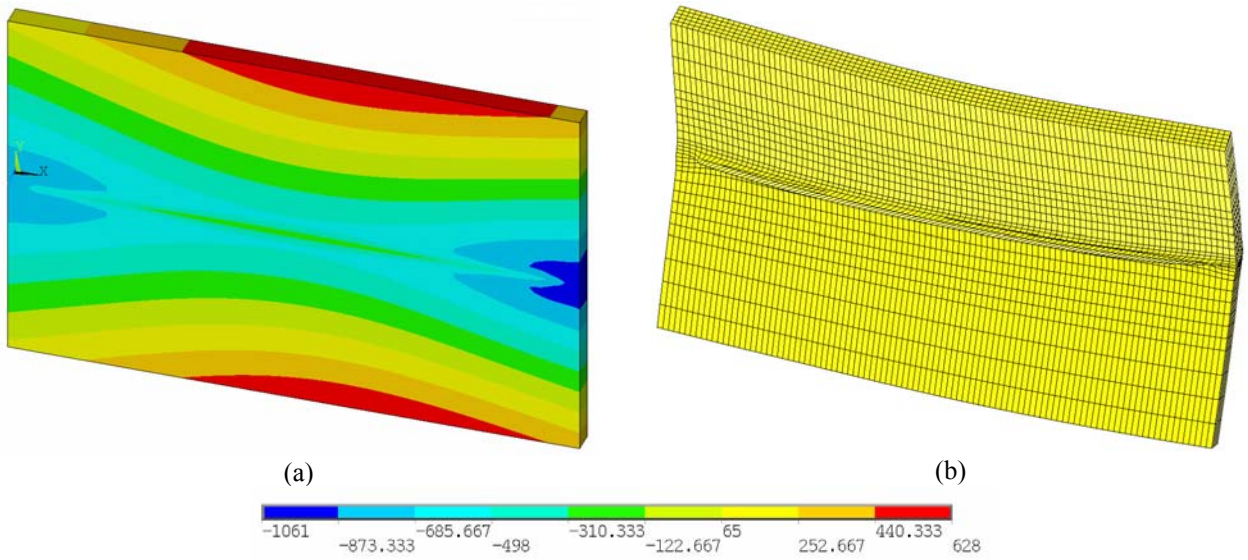

(a) (b)

Figure 7. (a) Residual transverse displacement field (in μm) and (b) final deformed shape (amplified 20×).

The residual stress field is illustrated in Fig. 8 on *x* (longitudinal) and *y* (transversal) directions as a contour plot. As expected, it is confirmed the occurrence of high tensile stresses in the longitudinal direction near the weld bead. In the transverse direction, it is observed high compressive stresses near the start and end points of the bead.

A comparison between the numerical and experimental stresses, analyzed at section x=150 mm, is shown in Fig. 9. It can be seen that, for stresses in the longitudinal direction (Fig. 9a), there is a good agreement between both sets of results only for the points farther than 20 mm from y=0. However, this can be explained by the fact that the experimental technique used is X-ray diffraction, which, according to Cullity (1978), does not indicate a true stress in points where plastic strain has occurred, which is the case near the fusion line.

For stresses in the transversal direction (Fig. 9b), it is verified an inconsistency between the results for points far away from y=0. Nevertheless, the experimental results present a compressive stress of about 100 MPa on the plate edge, where is known that the transversal stress should be zero (because it is perpendicular to a free edge). Consequently, there is an uncertainty about the experimental measures of residual stresses, which is confirmed by Depradeux (2004). Thus, the numerical results obtained can be considered satisfactory.

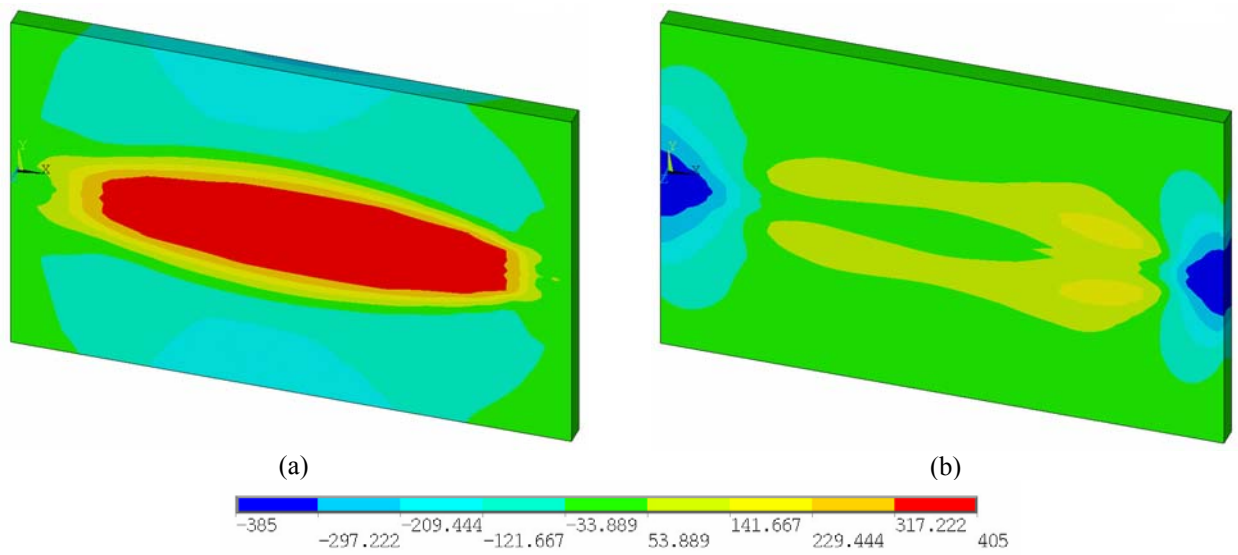

Figure 8. Residual stress field on longitudinal (a) and transversal (b) directions (in MPa).

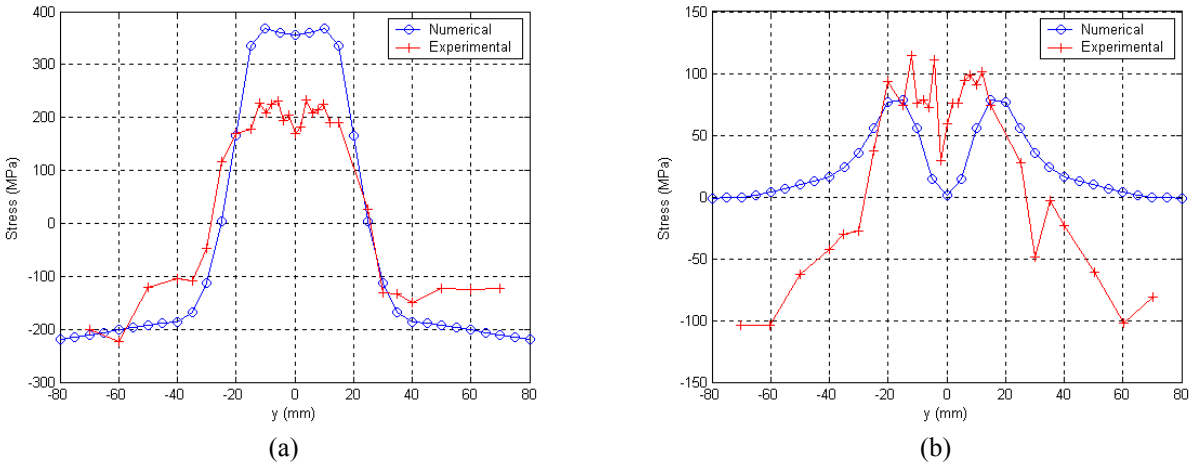

Figure 9. Residual stresses on bottom face on longitudinal (a) and transversal (b) directions at section x=150mm.

5. Conclusions

This study presented the structural analysis of a TIG welding without filler metal of a stainless steel AISI 316L plate. FEM was used to get the transient thermal stress and residual stress fields and distortions, based on the temperature time-history obtained through a previous thermal analysis. Thus, the two companion papers fully describe the modeling procedures necessary to carry out the complete simulation of welding-induced residual stresses and distortions. In general, the results of numerical simulations have shown to be in satisfactory agreement with experimental ones provided in the literature. In this comparison, the limitations of the experimental procedure must be taken into account and one can conclude about the feasibility and accuracy of the modeling procedure adopted, which is based in a series of simplifying assumptions and a set of parameter values used as inputs in both the thermal and structural analyses. It is believed that the modeling procedure described herein can be successfully extended to simulate other welding processes and the welding of parts with more complex geometries, although more specialized software could be more adequate for this purpose.

6. Acknowledgements

The authors wish to thank the agencies CNPq, of the Brazilian Ministry of Science and Technology, and CAPES, of the Brazilian Ministry of Education, for the grant of doctorate and research scholarships. The support of agency FAPEMIG through Project TEC1634/04 is greatly appreciated and acknowledged.

7. References

ANSYS, 1997, Theory Reference Manual, release 5.4.

Bezerra, A.C., Rade, D.A. and Scotti, A., 2005, “Finite Element Simulation Of Tig Welding: Thermal Analysis”, 18th International Congress of Mechanical Engineering, November 6-11, Ouro Preto – MG – Brazil.
Cullity, B.D., 1978, “Elements of X-Ray Diffraction”, 2nd edition, Addison-Wesley Publishing Company, Inc.
Depradeux, L., 2004, “Simulation Numerique du Soudage – Acier 316L – Validation sur Cas Tests de Complexite Croissante”, Ph.D Thesis, Ecole Doctorale des Sciences de L’Ingenieur de Lyon, L’Institut National des Sciences Appliquees (INSA) – Lyon.
Francis, J.D., 2002, “Welding Simulations of Aluminum Alloy Joints by Finite Element Analysis”, MS Thesis, Virginia Polytechnic Institute and State University.
Free, J.A. and Goff, R.F.D.P., 1989, “Predicting Residual Stresses in Multi-Pass Weldments with the Finite Element Method”, Computers and Structures, vol. 32, n. 2, pp. 365-378.
Fricke, S., Keim, E. and Schmidt, J., 2001, “Numerical Weld Modeling – a Method for Calculating Weld-Induced Residual Stresses”, Nuclear Engineering and Design, vol. 206, pp. 139-150.
Hong, J.K., Tsai, C.-L. and Dong, P., 1998, “Assessment of Numerical Procedures for Residual Stress Analysis of Multipass Welds”, Welding Journal, vol. 77, n. 9, pp. 372-382.
Kamtekar, A.G., 1978, “The Calculation of Welding Residual Stresses in Thin Steel Plates”, International Journal of Mechanical Sciences, vol. 20, pp. 207-227.
Lemaitre, J. and Chaboche, J. L., 1988, “Mécanique des Matériaux Solides”, Dunod, 2nd edition.
Murthy, Y.V., Rao, G.V. and Iyer, P.K., 1996, “Numerical Simulation of Welding and Quenching Processes using Transient Thermal and Thermo-Elastic-Plastic Formulations”, Computers and Structures, Vol. 60, No. 1, pp. 131-154.
Papazoglou, V.J. and Masubuchi, K, 1982, “Numerical Analysis of Thermal Stresses during Welding Including Phase Transformation Effects”, Journal of Pressure Vessel Technology, vol. 104, pp. 198-203.
Parlane, A.J.A., Allen, J.S., Harrison, J.D., Leggatt, R.H., Dwight, J.B., Bailey, N., Procter, E. and Saunders, G.G., 1981, “Residual Stresses and their Effect ”, The Welding Institute, U.K.
Rosenthal, D., 1941, “Mathematical theory of heat distribution during welding and cutting”, Welding Journal, N. 20, pp. 220-234.

8. Responsibility notice

The authors are the only responsible for the printed material included in this paper.